SHIELDING EFFECT OF HELIUM VESSEL IN CALCULATING AC LOSSES IN SUPERCONDUCTING MAGNETS

Moriyama, Shin-ichi
Research Institute for Applied Mechanics, Kyushu University : Graduate Student

Kawasaki, Shoji
Research Institute for Applied Mechanics, Kyushu University : Technical Assistant

Nakamura, Yukio
Research Institute for Applied Mechanics, Kyushu University : Associate Professor

Itoh, Satoshi
Research Institute for Applied Mechanics, Kyushu University : Professor

https://doi.org/10.5109/6779702

出版情報：Reports of Research Institute for Applied Mechanics. 31 (97), pp.1-13, 1983-09. 九州大学応用力学研究所
バージョン：

Reports of Research Institute for Applied Mechanics
Vol. XXXI, No. 97, 1983

SHIELDING EFFECT OF HELIUM VESSEL IN CALCULATING AC LOSSES IN SUPERCONDUCTING MAGNETS

By Shin-ichi MORIYAMA* , Shoji KAWASAKI† ,
Yukio NAKAMURA‡ and Satoshi ITOH§

Magnetic shielding effects of helium vessels surrounding superconducting toroidal magnets are investigated experimentally by using a model which simulates the helium vessel and the theoretical analysis is presented. It is shown that the rate of decay of pulsed external magnetic field is much smaller than that due to the well-known skin effect. We can estimate more accurately the ac losses in superconducting magnets by considering the shielding effects.

1. Introduction

Among fusion researchers, the need for superconducting magnets has been generally recognized from the relation between the fusion energy extracted from plasma and the electrical energy required for a magnet system. For tokamak devices, however, high-field superconducting magnets have been required and superconducting magnet technology has been advanced enough to ensure coils having such performance. The situation is now changing. Recent developments in magnet technology have enabled us to make high-field superconducting magnets, and there are some large fusion experiment programs using superconducting magnets[1),2)]. In applying superconducting magnets to tokamak devices, however, we are facing to a significant problem : Superconducting magnets are exposed to time-varying magnetic fields produced by the poloidal magnetic field coils and plasma disruptions. Under such conditions losses are generated in the superconductor due to changes in its magnetization and due to eddy currents in the stabilizing matrix, which is called 'ac losses'[3),4)]. Such losses can raise the temperature of superconductor enough to create a local normal zone. Thus, the resistive heating in a normal zone tends to cause the zone to propagate throughout the whole composite conductors. This complete reversion to the normal state is

* Graduate Student, Research Institute for Applied Mechanics, Kyushu University.
† Technical Assistant, Research Institute for Applied Mechanics, Kyushu University.
‡ Associate Professor, Research Institute for Applied Mechanics, Kyushu University.
§ Professor, Research Institute for Applied Mechanics, Kyushu University.

called a 'quench'. Therefore the ac losses must be accounted for in the design of any superconducting magnet system involving time-varying magnetic fields, and it is very important to establish the prediction method of ac losses.

We have been designing a new tokamak device (TRIAM-1M) whose toroidal magnetic field is supplied by the Nb_3Sn superconducting magnets. The Nb_3Sn superconductor is pool-cooled with the liquid Helium. The ac losses in the Nb_3Sn superconductor due to time-varying poloidal magnetic fields should be kept sufficiently low so as not to revert to the normal state on account of temperature increase. In the calculation of ac losses, the helium vessels which surround superconducting magnets has an important role by attenuating time-varying magnetic fields. Therefore, in order to make the exact evaluation of the ac losses the shielding effect should be taken into account.

In this paper, the shielding effect of helium vessel for time-varying magnetic fields by using a model which simulates that used in the TRIAM-1M device is investigated experimentally and the results are estimated analytically.

2. Experimental Setup

A model is made on a scale of about one-third for the helium vessel in the TRIAM-1M device. Major parameters of the model are listed in Table 1 together with those of the helium vessel. The material and the wall thickness of the model are selected so that the ratio of the thickness d to the skin depth δ is the same as that of the helium vessel, because it is expected that the decay of poloidal magnetic fields in the helium vessel can be estimated roughly using the skin depth :

$$\gamma = e^{-d/\delta} \tag{1}$$

where γ is the rate of decay, $\delta(=\sqrt{2\rho/\mu\omega})$ is the skin depth and ρ is the conductor resistivity.

The schematic diagram of the system measuring the pulsed magnetic field is shown in Fig. 1. The external pulsed field is generated by a discharge of the condenser bank through the dummy coil which simulates the poloidal field coil :

$$B_e(t) = B_o e^{-\alpha t} \sin \omega t \tag{2}$$

where α is the damping factor, $\omega(=\pi/2\tau)$ is the frequency and τ is the rise time. We use three condenser banks with capacitance values of 2 μF, 8 μFand 200 μF corresponding to the rise times of 6.9 μsec, 13.8 μsec and 70 μsec, respectively. The internal magnetic field in the model is picked up by magnetic probes. A signal of the magnetic probes is transmitted by a coaxial cable which is covered by a copper pipe so as to shield itself from the external pulsed field or the high-frequency noise. In estimating the ac losses we must calculate the time-varying rate of a pulsed field to which the superconductor is exposed, because the losses

Table 1. Major parameters of the model and the helium vessel in the TRIAM-1M device.

	Model	Helium vessel
Shape	Dee-shape	Dee-shape
Bore	145mm×223mm	440mm×670mm
Cross sectional shape	rectangle	rectangle
Cross section : $l_x \times l_y$	90mm×80mm	280mm×240mm
Conductor wall tickness : d	1.5mm	7mm～43mm
Conductor material	Cu	SUS
Condutor resistivity : ρ	$1.7\times10^{-8}\Omega$m(at 20℃)	$4.5\times10^{-7}\Omega$m(4.2K)
Ratio d/δ	$1.14\times10^{-2}/\sqrt{\tau}$	$1.04\times10^{-2}/\sqrt{\tau}$(d=7mm)

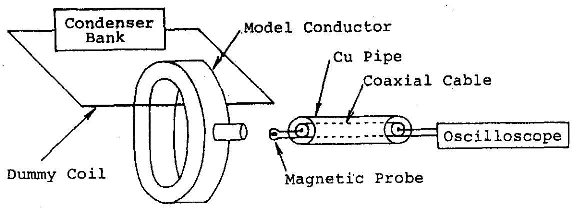

Fig. 1. Schematic diagram of the system measuring the pulsed magnetic field.

are proportional to the square of the rate. Therefore we define the rate of decay by

$$\gamma \equiv \frac{\text{maximum } dB_i/dt(\text{measured by the magnetic probes})}{\text{maximum } dB_e/dt(\text{calculated from Eq. (2)})} \quad (3)$$

where $B_i = B_i(x_p,y_p,z_p,t)$, $B_e = B_e(x_p,y_p,z_p,t)$ and x_p,y_p,z_p are the coordinates of measuring position.

3. Experimental results

A oscilloscope signal of the magnetic probe in the case of the external magnetic field with the rise time of 6.9 μsec is shown in Fig. 2. The rate of decay estimated from the first peak value of the signal is 7.3×10^{-4}. This value is much smaller than the rate ($\gamma = 1.4\times10^{-2}$) calculated from Eq. (1). The signal in Fig. 2, futhermore, is distorted as if a damped oscillation is superimposed on an exponential attenuation. These results suggest that the shielding effect of the helium vessel differs from the well-known skin effect.

Distributions of the rates of decay in the interior of the model is shown in Fig. 3. Here the subscripts // and $\perp$ express to be parallel to or perpendicular to the inner wall of the model, respectively. Both of $\gamma_{\parallel}$ and $\gamma_{\perp}$ do not depend remarkably on the distance X from the inner wall and the difference between them is small, nevertheless the external pulsed field varies spatially with respect to the direction and strength. This indicates that the shielding effect of helium vessel is not so much influenced by inhomogeneity of magnetic fields generated by poloidal coils.

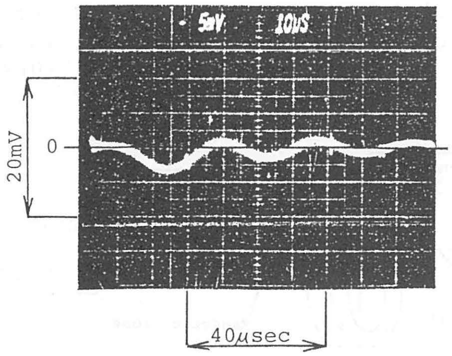

Fig. 2. Oscilloscope signal of the magnetic probe. The rise time τ of the external magnetic field is 6.9 μ sec.

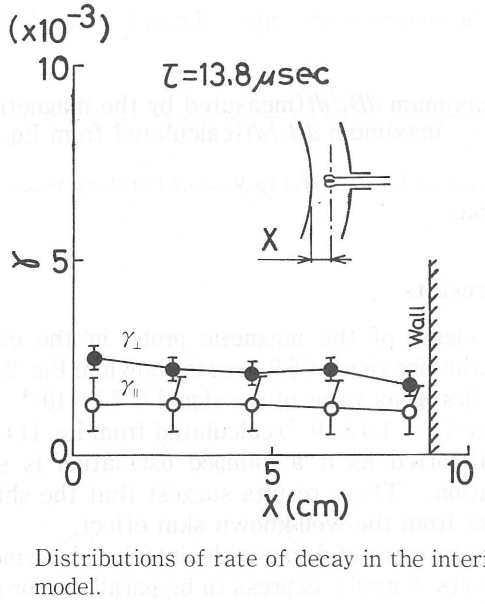

Fig. 3. Distributions of rate of decay in the interior of the model.

Figure 4 shows the dependence of rate of decay on the rise time of pulsed field. The rates of decay measured by the magnetic probe change exponentially with increasing the rise time. This dependence is similar to that of the broken line estimated from Eq. (1), but the values are smaller than the latter by one order as a whole. Thus, we should make the more strict estimation of the shielding effect of helium vessel as described in the following section.

4. Shielding effect of helium vessel

In order to estimate the shielding effect of helium vessel the diffusion equation governing the penetration of magnetic flux into a hollow conductor with arbitrary configuration should be solved for external pulsed fields (as experssed by Eq. (2)), but this solution is considerably complicated. So we make an analysis along the following procedures which include a few assumptions.

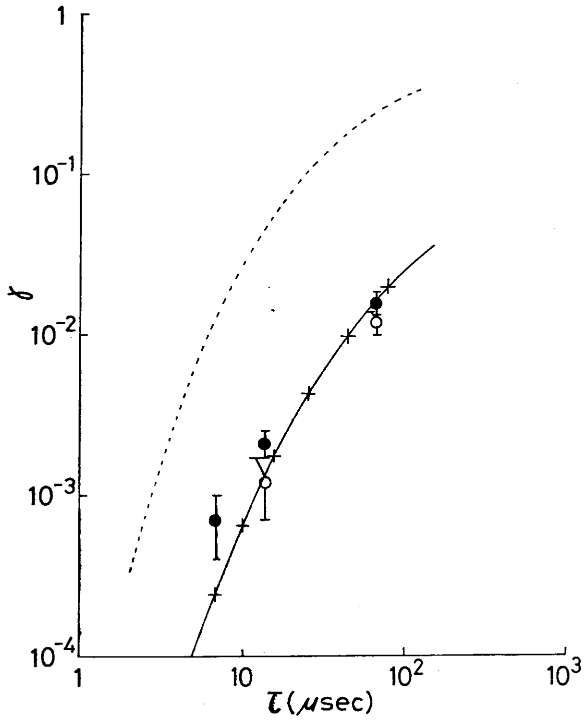

Fig. 4. Dependence of rate of decay on the rise time of pulsed magnetic field. The broken line shows the rate of decay due to the well-known skin effect, and the solid line and symbol + show the analytical results mentioned in the Section 4.

(1) The helium vessel is treated as a hollow cylindrical conductor illustrated in Fig. 5. The wall thickness and inner radius are equal to the thickness d or the equivalent radius $l_x l_y/(l_x+l_y)$, respectively, where d, l_x and l_y are listed in Table 1.

(2) The diffusion equation is solved for a steady state oscillation. The rate of decay is derived from the solution.

(3) Then, in order to obtain a transient solution for the external pulsed field we adopt a multi-layer cylindrical conductor illustrated in Fig. 6 as a computational model. The individual layer thickness is negligibly thin in comparison with the skin depth for the pulsed field. By using this model, the diffusion equation can be rewritten in the differential equation which does not include the terms of space derivative $\partial/\partial r$.

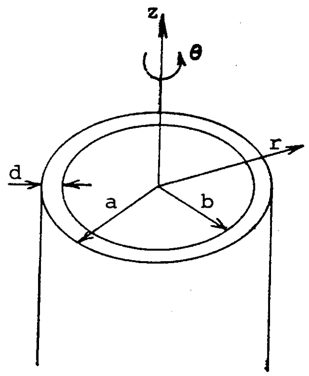

Fig. 5. Hollow cylindrical conductor employed for the analysis. Here a and b are the outer and inner radii of the conductor, respectively, and d is the conductor wall thickness.

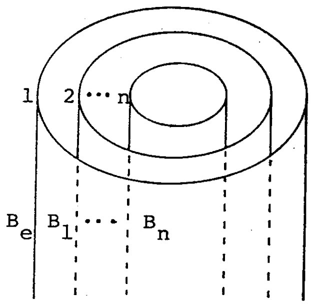

Fig. 6. Multi-layer cylindrical conductor adopted as a computational model.

(4) The differential equation is solved for the external pulsed field. The rate of decay in the procedure (2) is compared with that calculated from this transient solution so as to ascertain whether the shielding effect for external pulsed fields can be estimated using the steady state solution.

4.1. Steady state solution of the diffusion equation

The diffusion equation is given by

$$\nabla^2 \vec{B} = \frac{\mu}{\rho} \frac{\partial \vec{B}}{\partial t}. \tag{4}$$

If the time-oscillating term of magnetic field is assumed to behave sinusoidally, the time derivative $\partial/\partial t$ can be replaced by $i\omega$ and the diffusion equation becomes :

$$\nabla^2 \vec{B} + k^2 \vec{B} = 0 \tag{5}$$

where $k = \sqrt{-i\omega\mu/\rho} = (1-i)/\delta$.

We use the cylindrical coordinate (r, θ, z) illustsated in Fig. 5. The solution for magnetic field diffusion into the hollow conductor is derived for a field which is either parallel or perpendicular to the conductor axis[5),6)].

For a field parallel to the conductor axis the general solutions of Eq. (5) may be written by

$$B_z(r) = \begin{cases} B_o & \text{for } r \geqq a \\ AJ_0(kr) + CY_0(kr) & \text{for } a \leqq r \leqq b \\ AJ_0(kb) + CY_0(kb) & \text{for } r \leqq b \end{cases} \tag{6}$$

where A, C are constants and J_n, Y_n are the n-th order Bessel functions. The following boundary conditions are applied :

$$\text{at } r = a, \quad B_z(r) = B_0$$

$$\text{and at } r = b, \quad \oint E_\theta dl = -\frac{\partial}{\partial t} \int B_z ds.$$

Substituting these conditions in Eq. (6) results in the following experssion for the internal magnetic field :

$$B_i \equiv B_z(b) = \frac{4B_o}{\pi k^2 b^2} \frac{1}{D} \tag{7}$$

$$D = J_0(ka) Y_0(kb) - J_0(kb) Y_0(ka) + \frac{2}{kb} (J_0(ka) Y_0'(kb) - J_0'(kb) Y_0(ka))$$

where $J'(z) = \dfrac{dJ}{dz}$ and similarly $Y'(z) = \dfrac{dY}{dz}$.

On the other hand, for a field perpendicular to the conductor axis the general solutions may be expressed using the vector potential in the following equations :

$$A_z(r) = \begin{cases} (B_o r + \frac{C}{r})\sin\theta & \text{for } r \geqq a \\ (QJ_1(kr) + RY_1(kr))\sin\theta & \text{for } a \leqq r \leqq b \\ Pr \cdot \sin\theta & \text{for } r \leqq b \end{cases} \tag{8}$$

where C, Q, R and P are constants. From the boundary conditions of B_r and B_θ, at $r = a$ and $r = b$, the following equation is derived :

$$B_i \equiv P = \frac{4B_o}{\pi k^2 b^2} \frac{1}{F} \tag{9}$$

$$\begin{aligned} F = & \frac{1}{k^2 ab}(J_1(kb)Y_1(ka) - J_1(ka)Y_1(kb)) \\ & + \frac{1}{ka}(J_1(ka)Y_1'(kb) - J_1'(kb)Y_1(ka)) \\ & + \frac{1}{kb}(J_1(kb)Y_1'(ka) - J_1'(ka)Y_1(kb)) \\ & + J_1'(ka)Y_1'(kb) - J_1'(kb)Y_1'(ka) \end{aligned}$$

Usually, for a hollow conductor such as the helium vessel used in tokamak devices the equivalent radius b is sufficiently large in comparison with the wall thickness d. Therefore, Eq. (7) or Eq. (9) may be simplified by the application of the approximate formulas of the Bessel functions. In the case of a fast time-varying poloidal field the thickness d is larger than the skin depth δ, so the following formulas may be applied :

$$J_n(z) \simeq \sqrt{\frac{2}{\pi z}} \cos\left(z - \frac{(2n+1)\pi}{4}\right)$$

$$Y_n(z) \simeq \sqrt{\frac{2}{\pi z}} \sin\left(z - \frac{(2n+1)\pi}{4}\right).$$

Substituting in Eq. (7) and Eq (9) results in the following expression

$$B_i = B_o \Big/ \left(\cos(kd) - \frac{kb}{2}\sin(kd)\right). \tag{10}$$

Futhermore, Eq. (10) is approximately reduced to the form :

$$B_i = \frac{2B_o}{e^{(1+i)d/\delta}\left(1 - \frac{kb}{2i}\right)}. \tag{11}$$

From Eq. (11) the rate of decay of the fast time-varying magnetic field is newly defined by

$$\gamma = \frac{2\sqrt{2}\delta}{b}e^{-d/\delta}. \tag{12}$$

On the other hand, in the case of a slow time-varying poloidal field the thickness d is smaller than the skin depth δ. Thus, from the following formulas:

$$J_n(ka) \simeq J_n(kb) + kdJ_n'(kb)$$
$$Y_n(ka) \simeq Y_n(kb) + kdY_n'(kb)$$

both Eq. (7) and Eq. (9) is approximately reduced to the form:

$$B_i = \frac{B_o}{1+i\omega\tau_s} \tag{13}$$

where $\tau_s (= \mu bd/2\rho)$ is the skin time governing the penetration of a vertical magnetic field into a shell[7]. From Eq. (13) the rate of decay of the slow time-varying magnetic field is the form:

$$\gamma = 1/\sqrt{1+\omega^2\tau_s^2} \tag{14}$$

4.2. Transient solution for a pulsed field

The differential equations governing the penetration of magnetic flux into a multi-layer cylindrical conductor illustrated in Fig. 6 may be written by

$$\begin{aligned}
B_e &= B_1 + c_{11}\frac{dB_1}{dt} + c_{12}\frac{dB_2}{dt} + \cdots + c_{1n}\frac{dB_n}{dt} \\
B_1 &= B_2 + c_{22}\frac{dB_2}{dt} + c_{23}\frac{dB_3}{dt} + \cdots + c_{2n}\frac{dB_n}{dt} \\
&\cdots \\
B_{n-1} &= B_n + c_{nn}\frac{dB_n}{dt} \\
B_n &= B_i
\end{aligned} \tag{15}$$

where $c_{mk}(m,k = 1,2,\cdots,n)$ are constants and $B_k(k = 1,2,\cdots,n)$ is a magnetic field on the inner surface of k-th layer. Equation (15) is reduced to a differential equation:

$$B_e = B_i + a_1\frac{dB_i}{dt} + \cdots + a_n\frac{d^nB_i}{dt^n} \tag{16}$$

where $a_k(k = 1,2,\cdots,n)$ are constants. This is the approximate equation of the diffusion equation given by Eq. (4). Since the steady state solution in Eq. (15) must coincide with Eq. (10) or Eq. (13), we can determine the constant a_k from the comparison between both of them:

$$a_k \simeq \left(\frac{\mu}{\rho}\right)^k \frac{d^{2k-1}}{(2k-1)!}\frac{b}{2}. \tag{17}$$

In order to obtain the solution for the pulsed field expressed by Eq. (2) we apply Laplace transformation to Eq. (16):

$$\tilde{B}_i = \frac{B_o}{(s+\alpha)^2+\omega^2}\sum_k^n \frac{C_k}{(1+\tau_k s)} \tag{18}$$

where

$$\tau_k \simeq \begin{cases} \dfrac{\mu}{\rho}\dfrac{bd}{2}(=\tau_s) & \text{for } k=1 \\ \dfrac{\mu}{\rho}\dfrac{d^2}{(2k-1)(2k-2)} & \text{for } k \neq 1 \end{cases}$$

$$C_k = \frac{\tau_k^{n-1}}{\prod_{m\neq k}^{n}(\tau_k-\tau_m)}.$$

Consequently, the solution is expressed by

$$B_i(t) = \sum_k^n B_o C_k \left\{ \frac{\tau_k\omega \exp(-t/\tau_k)}{(1-\alpha\tau_k)^2+(\tau_k\omega)^2} - \frac{e^{-\alpha t}\cos(\omega t+\delta_k)}{\sqrt{(1-\alpha\tau_k)^2+(\tau_k\omega)^2}} \right\} \tag{19}$$

where $\delta_k = \tan^{-1}((1-\alpha\tau_k)/\omega\tau_k)$, and the signal of magnetic probe is defined as the form:

$$V_i(t) \equiv -\frac{dB_i}{dt}/\omega B_o. \tag{20}$$

In Eq. (19) the first term into the blanket{ } is due to the transient magnetic field at the first rise of external pulsed field, and it causes the signal to distort as mentioned in the previous section.

5. Analytical results and discussions

In order to compare the experimental results with the analytical results, we have carried out calculations of Eq. (20) for external pulsed fields with the various rise times. The computational results, together with oscilloscope signals of magnetic probe, are shown in Fig.7. From this figure we can find the good agreements with respect to the phase shift or the distortion in the wave forms. Regarding the rate of decay, we can also find from Fig. 4 that the theoretical values are in good agreement with the experimental values. Here the symbol + shows the rate of decay calculated from Eq. (20) and the fitting curve (solid line) shows that defined by Eq. (12). Therefore, the shielding effect of helium vessel for a transient magnetic field may be estimated from the rate of decay derived from the steady state solution described in the previous section.

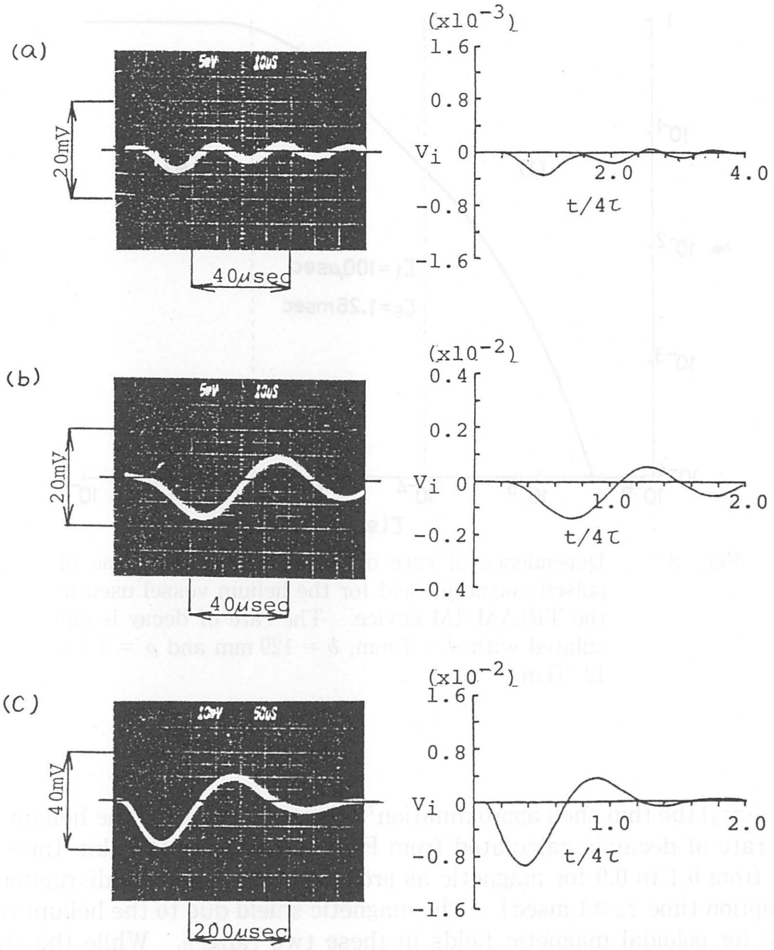

Fig. 7. Oscilloscope signals of the magnetic probe for the pulsed magnetic fields with (a) τ = 6.9 μsec, (b) τ = 13.8 μsec and (c) τ = 70 μsec, and the corresponding analytical results.

Figure 8 shows the dependence of rate of decay on the rise time of the pulsed magnetic field for the helium vessel used in the TRIAM-1M device. Here the characteristic time τ_t in this figure is defined by the rise time at which d/δ is unity. In the range I(the rise time $\tau < \tau_t$) the skin effect contributes the decay of magnetic fields, and the rate of decay is calculated from Eq. (12) by using the skin depth δ. It is smaller than 5×10^{-2} for magnetic field (with the rise time τ = 20 μsec~100 μsec) as generated by the turbulent heating coils. In the range

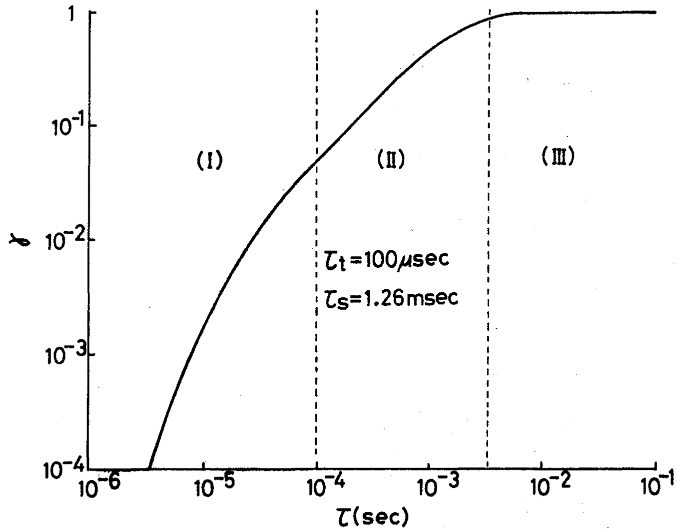

Fig. 8. Dependence of rate of decay on the rise time of pulsed magnetic field for the helium vessel used in the TRIAM-1M device. The rate of decay is calculated with d = 7 mm, b = 129 mm and $\rho = 4.5\times 10^{-7}\Omega$ m.

II($\tau_t<\tau<\pi\tau_s$) the thin shell approximation[7] can be applied for the helium vessel, and the rate of decay is calculated from Eq. (14) by using the skin time τ_s. It changes from 0.1 to 0.9 for magnetic as produced by the plasma disruption (with the disruption time $\tau_d\geq 1$ msec). The magnetic shield due to the helium vessel is effective for poloidal magnetic fields in these two ranges. While the shielding effect can be neglected in the range III ($\tau>\pi\tau_s$) which involves magnetic fields (with the rise time $\tau>10$ msec) generated by the control coils regulating the position and configuration of plasma column.

6. Conclusions

In order to make the exact evaluation of ac losses in superconducting magnets, the shielding effect of helium vessel for pulsed magnetic fields has been investigated experimentally. We have found that the results can be estimated analytically from the steady state solutions for magnetic field diffusion into a hollow cylindrical conductor. By this analysis the prediction method of ac losses becomes more accurate. The analytical results are being used in the design of the superconducting magnets for the TRIAM-1M device.

References

1) Haubenreich, P. N., Lubell, M. S., Cornish, D. N. and Beard, D. S., Nuclear Fusion 22 (1982) 1209.
2) Ivanov, D. P., Keilin, V. E., Stavissky, B. A. and Chernoplekov, N. A., IEEE Transactions on Magnetics MAG-15 (1979) 550.
3) Morgan, G. H., Journal of Applied Physics 41 (1970) 3673.
4) Carr Jr., W. J., Journal of Applied Physics 45 (1974) 929.
5) Khalaf-Allah, K., CLM-R 141 (1974).
6) Kriezis, E. E. and Tegopoulos, J. A., IEEE Transactions on Magnetics MAG-11 (1975) 1529.
7) Mukhovatov, V. S. and Shafranov, V. D., Nuclear Fusion 11 (1971) 605.

(Received June 30, 1983)